Influence of Laser-Induced Bubble Formation on Laser Chemical Machining

Atul[1*], Avaya Kumar Baliarsingh[2],
[1*]Associate Professor, Department of Mechanical Engineering, Nalanda Institute of Technology, Bhubaneswar, Odisha, India
[2]Assistant Professor, Department of Mechanical Engineering, Nalanda Institute of Technology, Bhubaneswar, Odisha, India

*Corresponding author e-mail: atul@thenalanda.com

Abstract

A non-traditional processing technique called laser chemical machining (LCM) provides very accurate and exact ablation of metallic surfaces. Laser-induced heat activation of chemical interactions between electrolytes and a metallic surface leads to material ablation. Large variations in ablation quality, however, can happen when LCM is used to prepare metallic surfaces because to rising bubbles. It has not been looked into how bubble formation during laser chemical machining affects the quality of the ablation. Ablation tests on titanium and ceramic under various thermal process settings were carried out for a more thorough analysis of the bubbles. High-speed camera equipment was used to capture the studies. Using Matlab, the video sequences were evaluated. The size and frequency of the generated bubbles were examined. The findings demonstrate that both materials developed boiling bubbles during processing. Titanium also generates smaller bubbles, which can be distinguished from one another as process bubbles based on their size. Additionally, as both boiling bubbles and process bubbles were found during machining within the process window, it was discovered that undisturbed laser chemical ablation can be accomplished in the presence of a boiling process.

Keywords

Micro Machining, Laser Micro Machining, Laser Chemical Removal,Nucleate Boiling, Highspeed Videography

1. Introduction

Constantly smaller components increase the demands of industrial manufac- turing processes. Traditionally used manufacturing processes are increasingly reaching their limits in terms of complexity and size [1]. Alternative machining processes, especially for metal workpieces, are the so-called non-conventional machining processes. Non-conventional machining processes are alternative machining processes, especially for metal workpieces and among them, laser chemical machining (LCM) is very important [2]. Laser chemical machining combines the advantages of laser processing, such as precise and localized energy input, and the advantages of electrochemical processing with a gentle energy impact without significant heat impact [3], which is why the unprocessed microstructure of the materials is not affected [4].

In laser chemical machining, the workpiece is irradiated by a laser, which in- troduces local, precise and adequate energy in the form of heat into the work- piece. The workpiece is surrounded by electrolytes [5]. Depending on the laser intensity applied and the spot size of the laser, the induced temperature fields on the workpiece change the electrochemical potential that an anodic material dis- solution is induced resulting in a material removal at the surface of the work- piece [6]. Within a suitable process window, a gentle ablation is generated without a de- tectable heat-affected zone and without remelting processes in the material, which is the main advantage of laser chemical machining compared to other la-ser based non-conventional ablation processes [4].

The process window of the laser chemical machining is strongly influenced by a variety of parameters [7], such

as laser power, flow rate of the electrolyte, machin- ing speed that is why irregularities of the ablation can occur when leaving the process window [8]. Since laser chemistry is mainly a temperature-dependent process, the quality of the ablation generated is mainly dependent on electrolyte boiling, along with the boiling bubble size and the dynamic behavior of the boil- ing bubbles [9].

In this work, the formation and the behavior of the bubbles are therefore examined more closely in order to identify the relationship between bubble formation and ablation quality. First, ablations with a variation of the process parameters, e.g. laser power and machining speed, are generated and recorded by a high-speed camera. The recorded videos are then analyzed with a focus on the bubble diameter, the adhering time of the bubbles on the workpiece and the bubble size after the bubble has detached from the workpiece.

Experimental Set-Up

A continuous-wave (cw) fiber laser with a wavelength of 1080 nm is used as the laser beam source. The Gaussian laser radiation is first collimated to a beam di- ameter of 8 mm, then further reduced to 2 mm by an inverted telescope and then focused with a lens system with a focal length of 53 mm. With this setup a focus diameter of 30 µm was realized.

Titanium 3.7024 was selected as treatment material, with a size of 20 mm × 20 mm × 1 mm. Ceramic (Al2O3) with a comparable absorption, surface quality and heat conductivity were selected as reference material, see Table 1. Reason for

this is that the surface quality is crucial for the number of nuclei. This means that more nuclei are formed in the recess on rougher surfaces. In addition, the absorption determines how much thermal power is introduced into the work- piece. The resulting temperature field correlates directly with the number of bubbles and the bubble diameter.

Table 1. List of material properties.

Parameter	Unit	Titanium	Ceramic
Surface quality S_a	µm	1.47	1.47
Heat conductivity λ	W/(mK)	22	23
Absorption	-	0.43	0.41

The laser powers were chosen in such a way that they cover all three regimes, no removal, non-disturbed removal and disturbed removal, of laser chemical material processing [7]. The workpieces were embedded in a closed chemical cell through which a 5 molar phosphoric acid was constantly flowing as electrolyte, see Figure 1. The flow rate of the acid was 3 m/s. The electrolyte height of approx. 20 mm on the workpiece impairs the power density of the laser beam on the workpiece with a transmission of 0.68. During the experiments the movement of the laser processing head was ensured by x- and y-axes. For investigations linear ablation lines were generated with velocities of 50 µm/s and 100 µm/s, see Table 2.

A high-speed camera including a band pass filter was used to record the inte- raction zone between the electrolyte and the workpiece during the process, compare Figure 1. The shadow method was used for video recording. It de- scribes a transmitted light method in which refractive index changes are made visible in transparent shadows, see Figure 2.

An illumination laser was used as the light source. The illumination unit con- sists of a pulsed diode laser with a wavelength of 810 nm, a widening optic for uniform illumination of the interaction zone.

The complete experimental set-up and the chosen experiment parameters are the same for all experiments, it is only varied in the laser power and the ma- chining speed, see Table 2 and Figure 1.

The high-speed images were taken with 256 × 256 pixels and frame rates of 22,000 frames per second. One camera pixel corresponded to a square surface with a side length of 1.75 µm. The video sequences were evaluated using Matlab.

As shown in the shadow images, Figure 2, the workpiece represents the lower dark area and the electrolyte represents the bright area due to its transparency. On the electrolyte side, induced transmission optical densities can now be de- tected during the process. The density differences show the forming bubbles and streaks. All the frames were individually separated and analyzed. The recorded images were first converted into binary formats and edges were detected, see Figure 2. The geometrically closed surfaces were assumed to be circular and evaluated as bubbles.

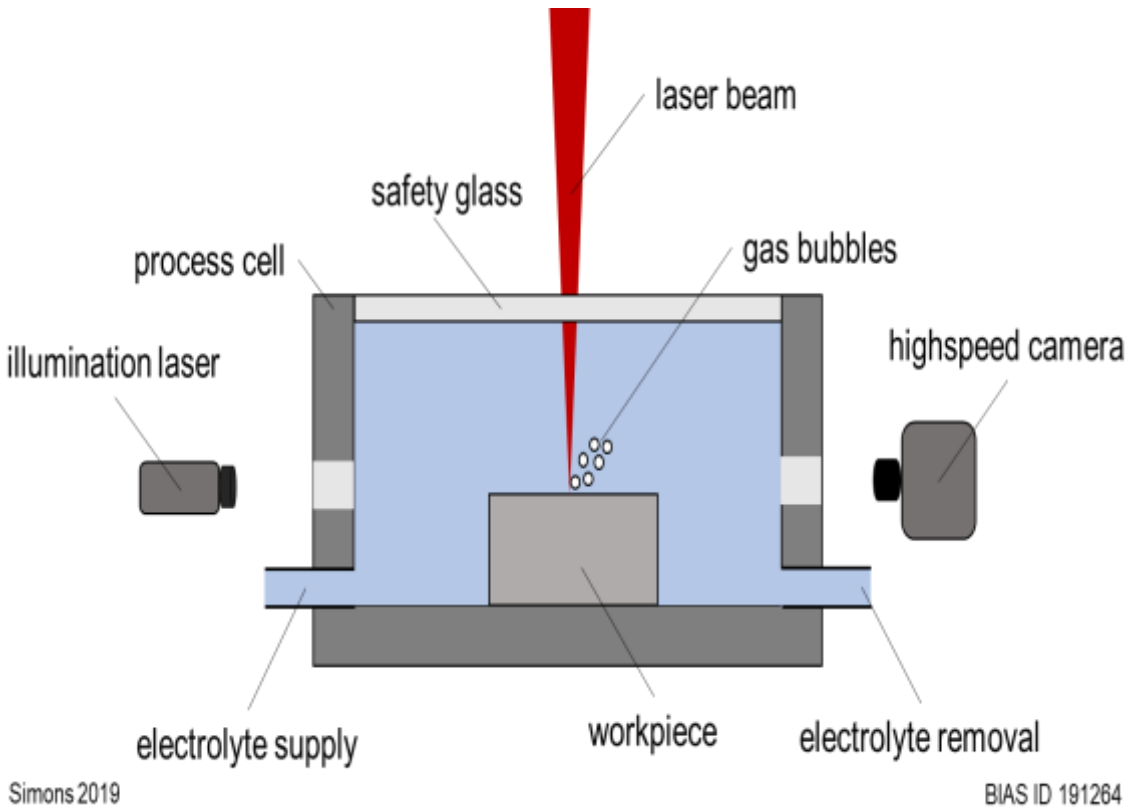

Figure 1. Schematic representation of the experimental set up.

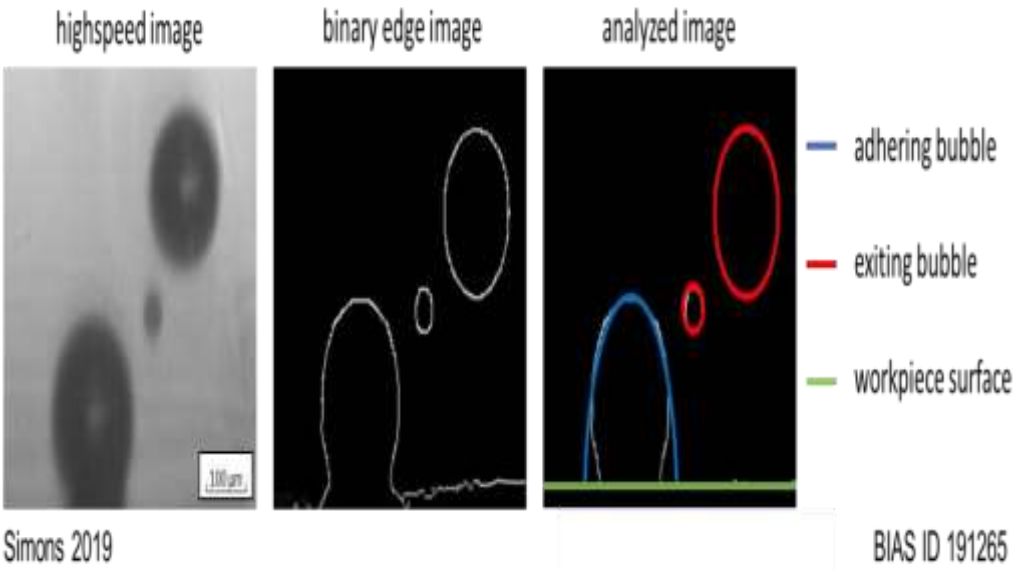

Figure 2. Presentation of the procedure for the analysis of high-speed video- graphy with the help of Matlab.

Table 2. List of process parameters used for experimental investigation.

	Parameter	Unit	Value
Laser beam (continuous wave)	wavelength	nm	1080
	laser power	W	0.6 ··· 1.8
	focus spot diameter	µm	30
	processing speed	µm/s	50 ··· 100
Phosphoric acid H_3PO_4	concentration	mol/L	5
	boiling temperature	˚C	104
	transmission coefficient	-	0.68
	layer height	mm	20
	flow speed	m/s	3

In the evaluation, a distinction was made between two types of bubbles, the adhering bubbles and the exiting bubbles. An adhering bubble was detected when the bubble was in direct contact with the workpiece surface. The bubble diameter of the adhering bubble was determined at the moment of detachment,so that the bubble diameter of adhering bubbles is equal to the maximum bubblediameter. An exiting bubble was determined when the bubble lost contact withthe workpiece and is at least 75 µm above the workpiece. The reason for this isthat the bubbles collapse after the ascent, so the bubble size of the exiting bub-bles was detected after the collapse. Before the collapse the bubbles have the same diameter as the adhering bubbles. Bubbles with a minimum diameter of 3 µm could be detected. In addition to the sizes, the number of both adhering andexiting bubbles was determined. With the help of the number of adhering bubbles and the recorded time period (5 s) the frequencies of the adhering bubbles were calculated. Additionally, the time in which the workpiece surface is covered with bubbles was determined (bubble

coverage time). For this purpose, the time was detected in which no bubble adheres to the surface of the workpiece in the area of the laser irradiation.

Influence of Laser Power on Bubble Formation

Based on the process parameters in **Table 2**, the average diameters of adheringand exiting bubbles were plotted in **Figure 3**.

As can be seen in **Figure 3**, with increasing laser power, the adhering bubble averages shift to larger bubble diameters, which in comparison mean that bub-bles with smaller diameters occur at lower laser powers. With the process para-meters shown in **Figure 3**, a minimum bubble diameter of 4 µm could be meas- ured and a maximum diameter of 271 µm.

If one considers the exiting bubbles based on **Figure 3**, the analyzed bubble diameters are essential smaller than those of the adhering bubbles. Moreover, itbecomes clear that the averages are almost similar for all laser powers. Hence they are independent of the laser power used.

Figure 4 shows some exemplary image sequences which illustrate the typical dynamics of bubble formation. The image sequences of low laser power clearly show that the bubble dynamics are very low. Compared to image sequences with higher laser power, the workpiece surface is covered with bubbles over shorter periods of time, which can also be seen in **Figure 5**. **Figure 5** shows the time during which the surface of the workpiece is covered with bubbles in relation tothe experimental time.

It can be observed that the growth time of the bubbles in the low laser power range is many times longer, see **Table 3**, a smaller quantity of bubbles is formed regarding to the processing time. The bubbles with a low diameter initially rise

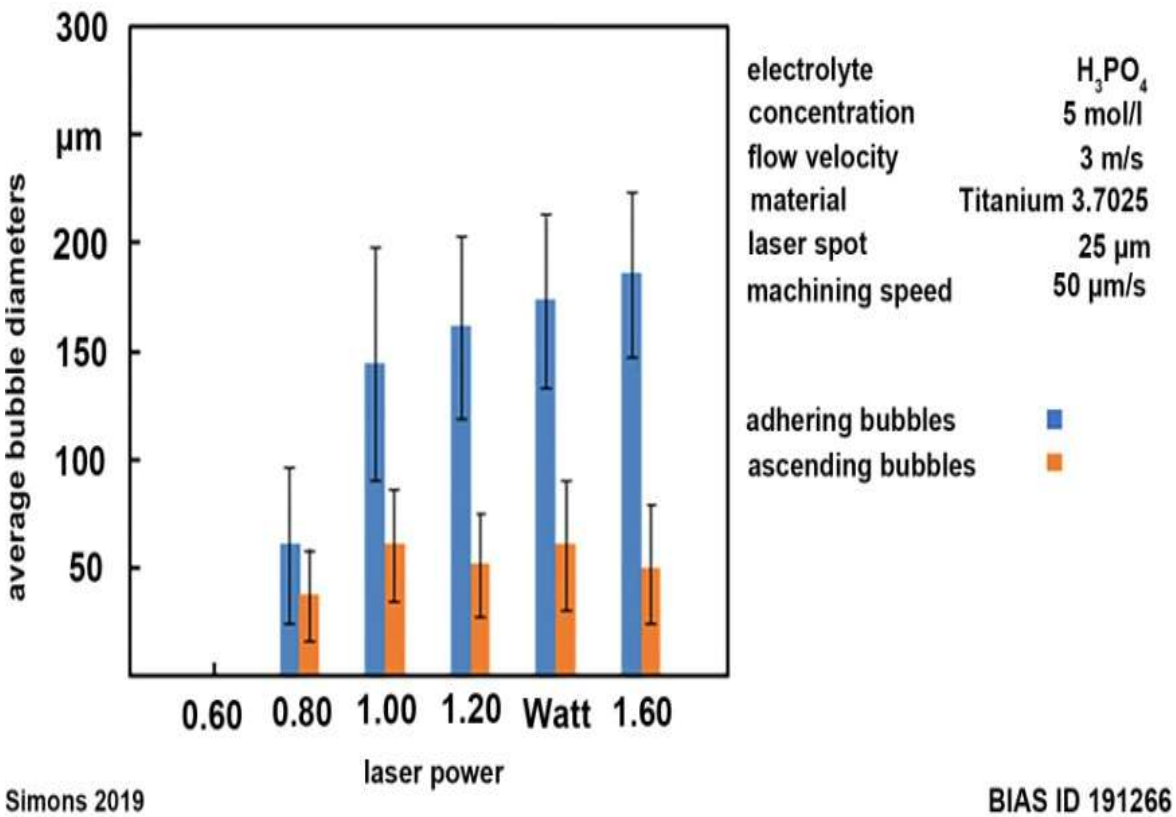

Figure 3. Representation of the average bubble diameters during laser chemicalmachining at a machining speed of 50 µm (Titanium).

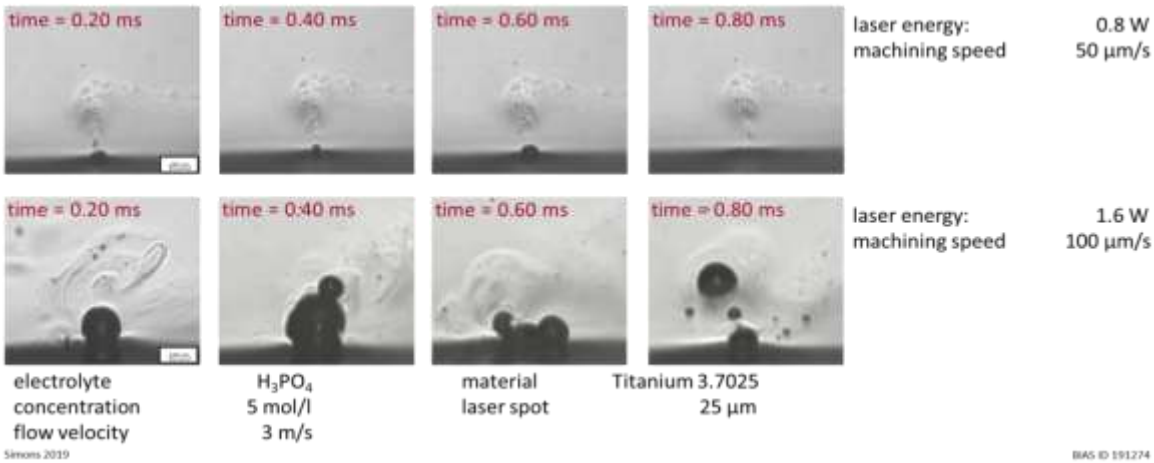

Figure 4. Formation of bubble at interaction zone with a machining speed of 50 µm/s (Titanium).

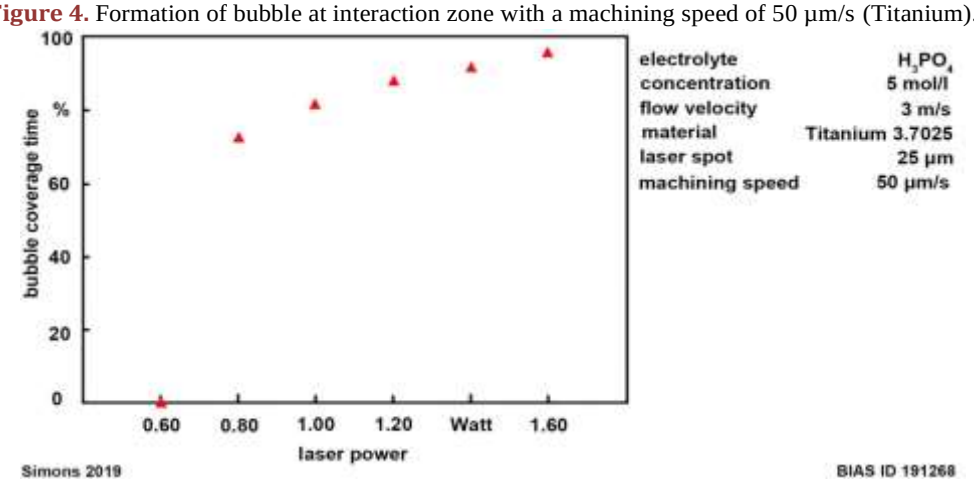

Figure 5. Evaluation of the time affected by bubbles and the time free of bubbles (Tita- nium).

Table 3. Evaluation of the number of adhering bubbles, exiting bubbles, formation fre- quency and surface temperature calculated according to [7] with a machining speed of 50 µm/s (Titanium).

laser power [W]	surface temperature [˚C]	number of adhering bubbles	number of exiting bubbles	frequency [1/s]
0.60	85	0	0	0
0.80	104	1053	5901	210.6
1.00	123	2261	12,159	452.2
1.20	148	3516	17,589	703.2
1.40	171	4615	26,002	923
1.60	192	5977	30,138	1195.4

vertically upwards, where they are captured by the flow at a certain height (200 µm) and transported away, as can be seen in **Figure 4**.

The bubbles of larger diameters collapse very quickly. This results in pressurewave. The collapsed bubble therefore divides into several small diameter bub-

bles. These resulting bubbles are detected as exiting bubbles. They act as nucleifor a new bubble formation or they are pushed away by the collapse pressure wave and transported away by the electrolyte flow. These processes are repeated over the entire processing time for both small and large diameter bubbles, butthey are not periodic.

At low laser powers the number of adhering bubbles and accompanied the formation frequency is much smaller compared to higher laser powers, see **Ta- ble 3**. **Table 3** shows the surface temperatures of the workpiece in the focal spot zone based on [7], assuming the simplification that the bubbles do not interfere with the absorption and thus do not influence the surface temperatures. As can be seen, this correlates directly with the laser power and thus also with the num- ber of bubbles.

A comparison of **Figure 3** and **Figure 6** shows the influence of the machining speed on bubble formation. The average value of adhering bubbles in **Figure 6** is in a much smaller diameter range than in **Figure 3**. The smallest measured adhering bubble diameter based on the process parameters in **Figure 6** is 3 µm and the largest measured diameter is 257 µm.

With the diameters of the exiting bubbles, there are no significant changes when the machining speed is increased.

Figure 7 shows that due to the smaller bubbles, the adhering time of the bub- bles relative to the experimental time is significantly reduced. As the laser power increases, however, the adhering time increases linearly as shown in **Figure 3**, as well.

If one compares the image sequences from **Figure 4** and **Figure 8**, one can see that the bubble size also increased with increasing laser power. This effect occurs independently of the machining speed. The image sequences clearly show that the dynamic behavior of the bubbles decreases significantly with increasing ma-chining speed.

A quantitative difference can be seen. A higher machining speed results in a lower number of boiling bubbles, which collapse and accordingly a lower num-ber of exiting bubbles is produced, see **Table 4**.

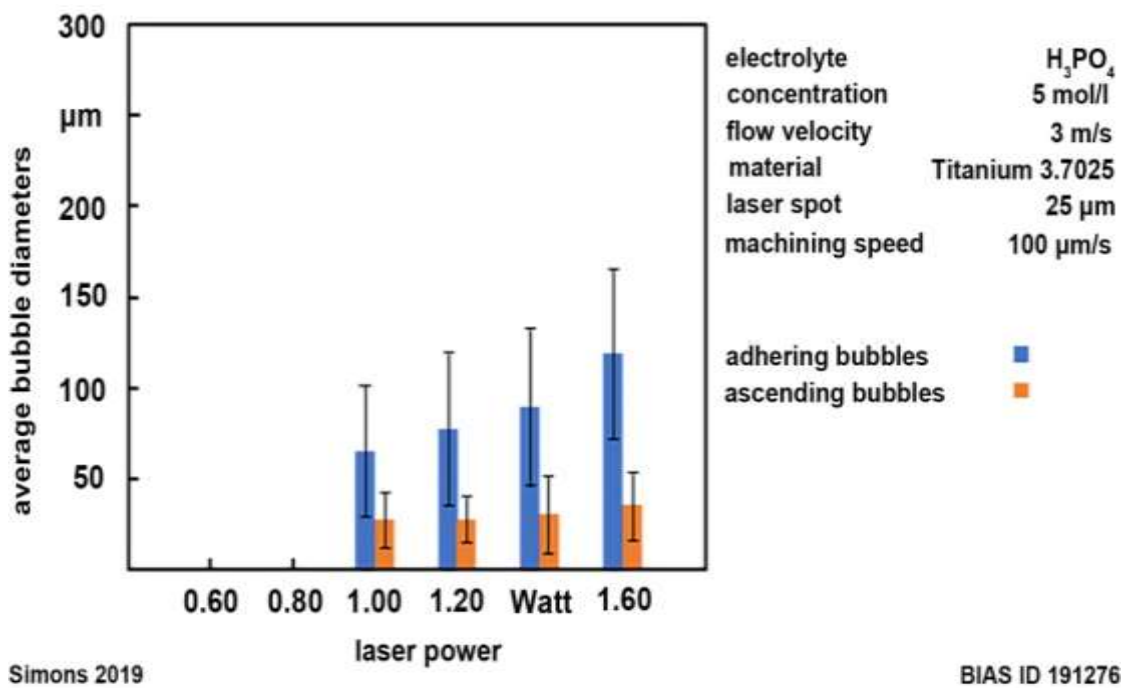

Figure 6. Representation of the average bubble diameters during laser chemicalmachining at a machining speed of 50 µm/s (Titanium).

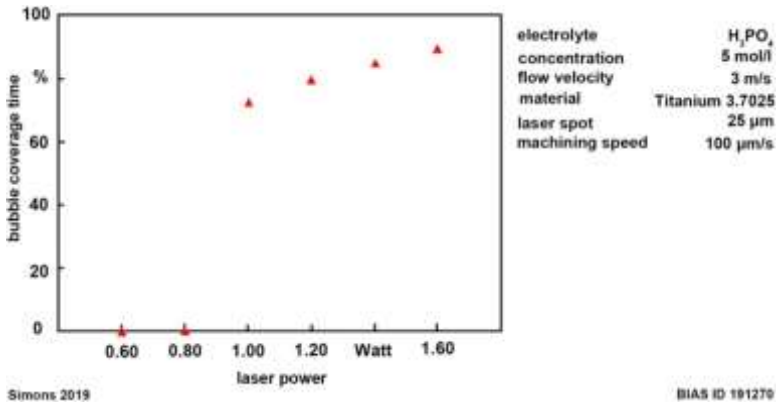

Figure 7. Evaluation of the time affected by bubbles and the time free of bubbles(Titanium).

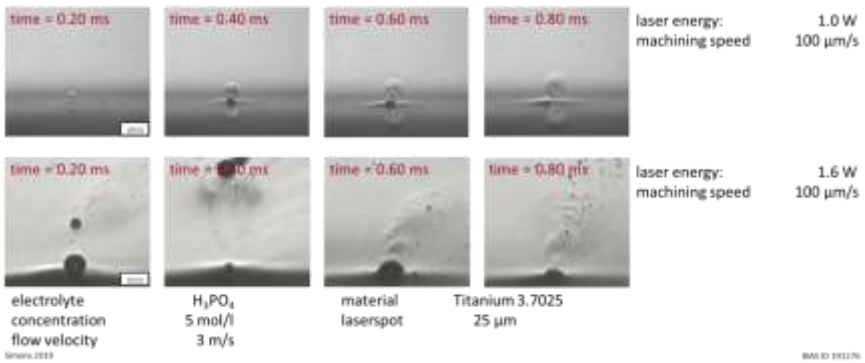

Figure 8. Formation of bubbles at interaction zone with a machining speed of 100 µm/s(Titanium).

Table 4. Evaluation of the number of adhering bubbles, exiting bubbles, formation fre-quency and surface temperature [7] with a machining speed of 100 µm/s (Titanium).

laser power [W]	surface temperature [˚C]	number of adhering bubbles	number of exiting bubbles	frequency [1/s]
0.60	85	0	0	0
0.80	104	0	0	0
1.00	123	1648	8654	329.6
1.20	148	2823	15,305	564,6
1.40	171	3702	21,641	740,4
1.60	192	5069	28,613	1013.8

Irrespective of the machining speed, the number of bubbles produced in-creases with the laser power.

Differences in Bubble Properties

To characterize the different bubbles inert Ceramic was irradiated additional toTitanium. In experiments with low laser powers (0.6 W and 0.8 W), no evaluable

bubbles were formed. An evaluation of experiments could be carried out only at higher laser powers, as shown in **Figure 9** and **Figure 10**. It is important to note that the Ceramic used has the same thermal conductivity as Titanium. For this reason, based on the calculations of [7], the surface temperatures of the Ceramic material are the same as those of Titanium, see **Table 2** and **Table 3**.

It is noticed that bubbles of larger diameter are produced by irradiating Ce- ramic. The smallest detected adhering bubble had a diameter von 75 µm. The largest measured diameter of adhering bubbles is 269 µm, which is comparableto the adhering bubble diameters on Titanium.

The observations at higher machining speeds are analogous to those for ma- chining Titanium, compare **Figure 6** and **Figure 11**. The time periods, in which the workpiece is free of bubbles see **Figure 12** are also similar to those shown in **Figure 7**. Even at a higher machining speed, no adhering bubble diameter below 75 µm was detected on Ceramic. The highest measured adhering bubble diame-ter is 262 µm, which is also comparable to the results shown before.

2. Discussion

In the LCM process, bubbles of different sizes are produced which reduce the ablation quality and thus represent a barrier to laser chemical machining [8]. Analogous to the assumptions in [9], different size ranges of the bubbles were detected during the machining of Ceramics and Titanium, compare **Figure 3** and **Figure 9**. This points to two different types of bubbles, process bubbles and boiling bubbles.

Process bubbles are formed due to the chemical reactions and are filled with hydrogen. These cannot be prevented during the laser chemical processing of metallic materials, such as Titanium, see **Figure 3**. The boiling bubbles are caused by the thermal influence of the laser on the workpiece surface, regardless of the workpiece material. The workpiece is heated in the interaction zone of the laser and the heat is transferred to the electrolyte. The boiling temperature of the

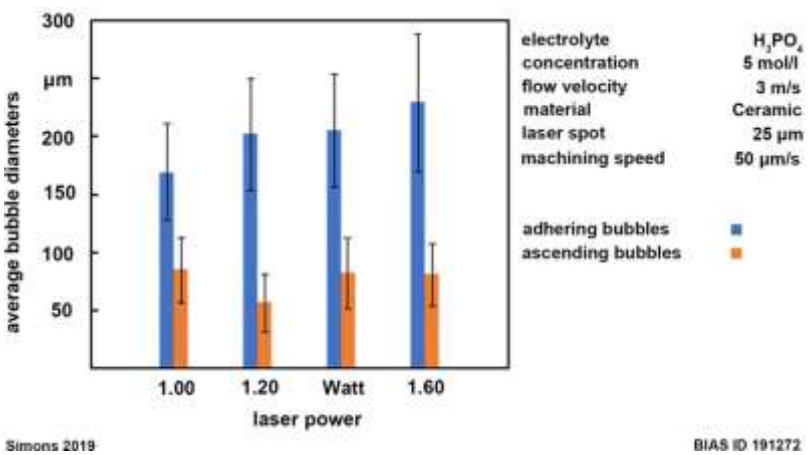

Figure 9. Representation of the average bubble diameters during laser chemicalmachining at a machining speed of 50 µm/s (Ceramic).

Figure 10. Evaluation of the time affected by bubbles and the time free of bub-bles (Ceramic).

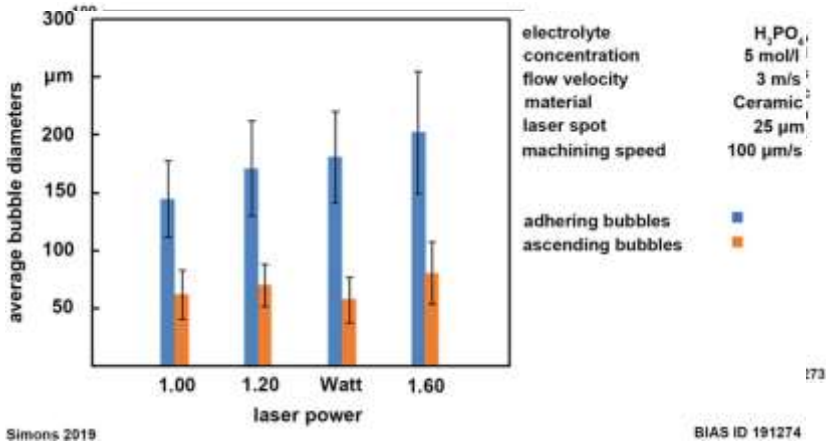

Figure 11. Representation of the average bubble diameters during laser chemi-cal machining at a machining speed of 100 µm/s (Ceramic).

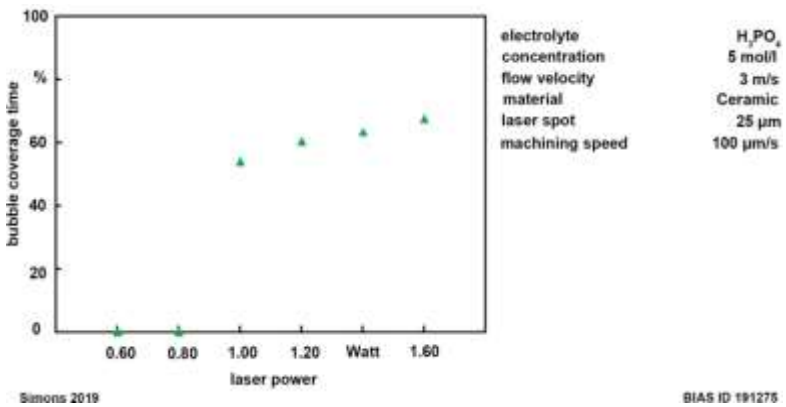

Figure 12. Evaluation of the time affected by bubbles and the time free of bub-bles (Ceramic).

electrolyte is locally exceeded, so that bubble boiling occurs. When looking at the bubble sizes during the heating of Ceramics, see **Figure 9**, it is noticeable that bubbles of larger diameters are formed compared to the machining of Titanium,see **Figure 3**. Since no process bubbles are formed during the heating of Ceramics,

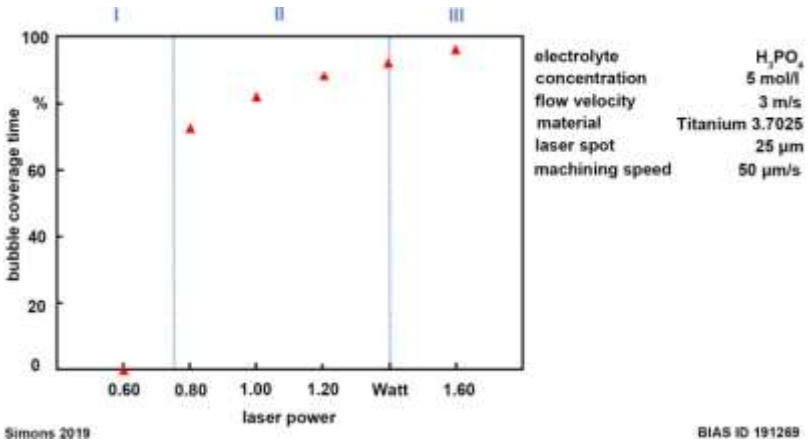

Figure 13. Representation of the time during which the workpiece surface iscovered by bubbles, including the removal regimes from [9].

it can be concluded that bubbles with smaller diameters are process bubbles and bubbles with large diameters are boiling bubbles.

As can be seen in **Figure 3** and **Figure 4**, high laser powers cause large di- ameters of adhering bubbles. This is due to the increased local temperature dis- tribution on the workpiece. In [8] there is a proportional relationship between the temperature on the workpiece and the laser power. Due to heat transfer me- chanisms, the electrolyte temperature also increases locally and a boiling process with increased bubble dynamics occurs.

If one considers the different processing regimes based on the definitions in [9], marked in **Figure 13**, no bubbles are formed if the ablation is not visible. Inthis case, the surface temperatures are not sufficient to locally break up the pas- sive layer and initiate the chemical reactions necessary for ablation. If the tem- perature of the laser power is calculated in the "no removal" regime, see **Table 3**, the boiling temperature of the electrolyte is not reached.

By increasing the laser power, the undisturbed area is reached. If the surface temperatures of the workpiece are higher than the boiling temperature, see **Ta- ble 3** and **Table 4**, local overheating of the electrolyte occurs, resulting in boiling bubbles.

If one looks at the recorded bubbles and the time in which the workpiece sur- face is covered by bubbles, see **Figure 3** and **Figure 13**, one can see that both thebubble size and the time in which the workpiece surface is covered by bubbles increases, so that a boiling process can be assumed. From this it follows that boiling bubbles are also present in the undisturbed state and thus undisturbed laser chemical processing under ambient conditions is possible if boiling bubbles are present.

If the laser power is further increased, the disturbed state is reached. It is visi- ble that due to a higher surface temperature, see **Table 3** and **Table 4**, the num- ber of boiling bubbles, the size of the boiling bubbles and the time in which the workpiece is covered by bubbles increases, see **Figure 3** and **Figure 13**. These can be seen analogously at a higher processing speed of 100 µm/s.

Looking at the regimes of undisturbed and disturbed ablation, the formation of boiling bubbles can be seen in both regimes. This indicates that bubble forma- tion and the boiling process itself is not an indication of the quality of ablation.

3. Conclusions

It could be shown that two different types of bubbles, process bubbles and boil- ing bubbles, occur during laser chemical processing, while the process bubbles do not affect the ablation quality.

Using video graphic analysis of bubble formation during chemical processing with the laser, it was shown that undisturbed ablation is possible even in the presence of boiling bubbles.

Acknowledgements

This work has been funded by the Project 403820352 “Steigerung der Prozesseffizienz der laserchemischen Bearbeitung durch Vermeidung der gasblasenbedingten Abtragsstörungen”. The authors gratefully acknowledge the financial support by the Deutsche Forschungsgemeinschaft.

Conflicts of Interest

The authors declare no conflicts of interest regarding the publication of this paper.

References

[1] Martin, A. and FitzGerald, B. (2013) Process over Platforms: A Paradigm Shift in Acquisition through Advanced Manufacturing, Center for a New American Securi-ty.

[2] Manjaiah, M., Narendranath, S. and Basavarajappa, S. (2014) Review on Non Con- ventional Machining of Shape Memory Alloys. *Transactions of Nonferrous Metals Society of China*, **24**, 12-21. https://doi.org/10.1016/S1003-6326(14)63022-3

[3] Eckert, S. and Vollertsen, F. (2018) Mechanisms and Processing Limits of Surface Finish Using Laser-Thermochemical Polishing. *Annals-Manufacturing Technology*,**67**, 201-204. https://doi.org/10.1016/j.cirp.2018.04.098

[4] Messaoudi, H., Böhmermann, F., Mikulewitsch, M., von Freyberg, A., Fischer, A.,Riemer, O. and Vollertsen, F. (2018) Chances and Limitations in the Application of Laser Chemical Machining for the Manufacture of Micro Forming Dies. 5*th International Conference on New Forming Technology*, **190**, 8. https://doi.org/10.1051/matecconf/201819015010

[5] Stephen, A., Lilienkamp, T., Metev, S. and Sepold, G. (1999) Laser-Assisted Micro- machining of Large-Area 3D Metallic Microparts. *Proc.* 1st *Int. Conf. Euspen* (ShakerVerlag), Bremen, May 31-4 June 1999, 20-23.

[6] Bäuerle, D. (2011) Laser Processing and Chemistry. Springer Verlag.https://doi.org/10.1007/978-3-64217613-5

[7] Mehrafsun, S. and Vollertsen, F. (2013) Disturbance of Material Removal in La-ser-Chemical Machining by Emerging Gas. *CIRP Annals*, **62**, 195-198. https://doi.org/10.1016/j.cirp.2013.03.030

[8] Messaoudi, H., Eckert, S. and Vollertsen, F. (2017) Thermal Analysis of Laser*Surface Engineering*, **5**, 685-691. https://doi.org/10.4236/msa.2017.810049

[9] Mehrafsun, S. and Messaoudi, H. (2018) Dynamic Process Behavior in Laser Chemical Micro Machining of Metals. *Journal of Manufacturing and Materials Processing*, **2**, 54-72. https://doi.org/10.3390/jmmp2030054